Radiative recombination of 2D electrons with nonequilibrium holes in silicon metal-insulator-semiconductor structures

I. V. Kukushkin and V. B. Timofeev

Institute of Solid State Physics, Academy of Sciences of the USSR
(Submitted 25 June 1986)
Zh. Eksp. Teor. Fiz. **92**, 258–278 (January 1987)

The recombination radiation of two-dimensional ($2D$) electrons as they recombine with injected holes in Si(100) metal-insulator-semiconductor structures has been studied. The shape of the emission line $2D_e$ as a function of energy is described by a step function. The width of this line is equal to the Fermi energy of the $2D$ electrons and increases linearly with the density of these electrons. This linear increase reflects a constancy of the state density of $2D$ electrons in the absence of a magnetic field. The recombination radiation of $2D$ electrons in the TO- and TA-phonon components of the spectrum is linearly polarized parallel to the $2D$ plane. The $2D_e$ line is observed to contract at densities corresponding to a transition from strong localization of the $2D$ electrons to metallization of these electrons. This transition is attributed to a screening of the random potential of defects. The kinetics of the structural changes in the depletion region in the presence of nonequilibrium electron-hole excitation and during illumination in the far-IR part of the spectrum has been studied. A method is proposed for determining the absolute value of the state density and the occupation numbers of the $2D$ electrons under conditions of strong localization. The state-density mass and the cyclotron mass have been determined: $M_d = (0.202 \pm 0.002)m_0$ and $m_c = (0.200 \pm 0.003)m_0$, respectively. The attenuation of one-particle excitations below the Fermi surface at the band bottom has been determined. The time scale of the recombination of the $2D$ electrons with photoexcited holes is $\approx 10^{-3}$ s.

§1. INTRODUCTION

The space-charge inversion layer in silicon metal-insulator-semiconductor (MIS) structures is the classical quasi-two-dimensional ($2D$) system, in which the properties of a $2D$ electron gas have been studied most completely.[1] Some questions which remain unsolved in this area concern the energy spectrum of these systems and are related for the most part to the density of localized and extended states and effects of the screening of the random potential of defects both with and without a magnetic field H. The electronic transport properties have so far been the main tool for experimental studies of these (and related) questions. Information on the state density is not extracted directly in experiments based on electronic transport. It is instead found by analyzing the measured behavior, fitting parameter values, and introducing assumptions which require special justification. Nevertheless, we know quite well that optical spectroscopy provides the most direct way for determining the energy distribution of the density of one-particle states. We have previously reported observing the radiation emitted by $2D$ electrons as they recombine with photoexcited holes in Si(100) MIS structures.[2] We have demonstrated that this method can be used to directly determine the energy distribution of the state density of $2D$ electrons in a perpendicular magnetic field.[3] In the present paper we present a complete description of this spectroscopic procedure. In particular, we discuss questions pertaining to the distributions of the charge and the electric field near the Si–SiO_2 interface during the injection of nonequilibrium electron-hole (e-h) pairs (§3). We also discuss the mechanism for radiative recombination (§4), the polarized optical properties in phonon (TO and TA) and no-phonon (NP) spectral replicas (§5) and the recombination kinetics (§8). The method proposed here has been used for experimental studies of the effects of screening of the random potential of defects (§6,7) and of the Fermi attenuation of one-particle excitations (§9).

§2. EXPERIMENTAL PROCEDURE AND STRUCTURES

In these experiments we used seven ordinary MIS transistors, fabricated on the (001) surface of p-type silicon. The structures have a semitransparent gate, with an area ranging from 0.3 to 5 mm^2 in different samples. We studied transistors both with a rectangular geometry, with five potential contacts for measuring the components ρ_{xx} and ρ_{xy} of the magnetoresistance tensor, and with the shape of a Corbino disk, for measuring the magnetoconductivity σ_{xx}. Nonequilibrium e-h pairs were generated with an LG-106 argon laser or an AL-107A GaAs light-emitting diode. In some cases, it was convenient to inject the nonequilibrium pairs across the p-n junction. A noteworthy point is that the experimental results do not depend on the e-h excitation method.

The experiments with the MIS transistors allowed us to carry out magnetotransport and spectroscopic measurements simultaneously and to compare the parameter values found by the various experimental procedures. The structures were fabricated under various technological conditions on different silicon wafers, in which the boron concentration N_A was varied from $5\cdot10^{14}$ cm^{-3} to $2\cdot10^{15}$ cm^{-3} and was determined from the dependence of the threshold voltage on the bias voltage on the substrate (§3). The seven structures which we studied differ markedly in quality; the maximum density of $2D$ electrons is found in the poorest structure: $\mu^* = 4\cdot10^3$ cm^2/(V·s) at $n_S^* = 9\cdot10^{11}$ cm^{-2} and $T = 1.5$ K. In the best structure we find $\mu^* = 3.1\cdot10^4$ cm^2/($V\cdot s$) at $n_S^* = 4\cdot10^{11}$ cm^{-2} and $T = 1.5$ K. The experiments are car-

 0038-5646/87/010146-11$04.00 © 1987 American Institute of Physics

ried out in an optical cryostat with a Faraday-geometry solenoid in fields up to 8 T. The spectral instrument is a DFS-12 double monochromator with a dispersion of 10 Å/mm in the working region. We wish to stress that the intensity of the recombination radiation of the 2*D* electrons which we were studying was exceedingly low. When we measured it in a photon-counting approach with a photomultiplier (*S-I* cathode), we obtained about 10 count/s. By way of comparison we note that the intensity of the bulk emission (*BE*) in lines of exciton-impurity complexes and of the electron-hole liquid is ~20 000 count/s. Furthermore, there is a *BE* line only 7 meV higher which is more intense by nearly three orders of magnitude. This situation requires a high-resolution spectral instrument (the resolution must be better than 0.5 meV) and a clean spectrum.

To measure the spectrum of such faint emission we use a signal buildup system (a multichannel analyzer), which substantially improves the signal-to-noise ratio. The spectra are processed numerically.

The magnetotransport measurements are carried out both at a direct current and at an alternating current with a frequency of 20 Hz. The magnitude of the measuring current is 10^{-7} A in the rectangular structures; the source-drain field in the Corbino-disk structures is less than 10^{-1} V/cm.

§3. CHARGE AND ELECTRIC FIELD DISTRIBUTIONS IN THE SEMICONDUCTOR

When a positive voltage V_g is applied between the potential contact and the metal gate of an MIS structure on the surface of *p*-type silicon, we know that the semiconductor will beocme negatively charged.[1] Part of this charge will be in the system of 2*D* electrons, and another part will be in a system of negatively charged acceptors, the depletion layer (Fig. 1b). At low values of V_g, the screening of the external electric field occurs exclusively as a result of the formation of the depletion layer. When the band curvature becomes comparable to the band gap of the semiconductor, a 2*D* channel appears. As V_g is raised further, there is no change in the

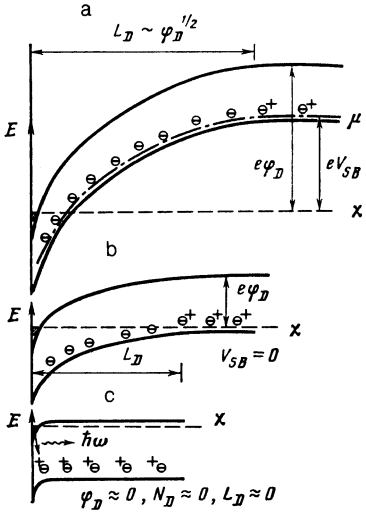

FIG. 1. Energy-band diagrams in *p*-types silicon with (a) negative, (b) zero, and (c) positive voltage on the substrate, V_{SB}. Case c also holds in the case of nonequilibrium excitation. Hatching—Region of the 2*D* electron channel; φ_D—band slope; L_D—thickness of the depletion layer; n_d—2*D* charge density in the depletion layer.

charge distribution in the depletion layer. The transition to an equilibrium charge distribution in the depletion layer occurs rapidly only at high temperatures ($T \sim 300$ K), for which thermal activation of charges from impurity centers into the band can occur easily. In contrast, at the low temperatures at which the present experiments were carried out ($T = 2$ K), this transition occurs extremely slowly (more on this below). It can, however, be accelerated by means of (for example) IR illumination, which has an effect similar to that of the temperature in that it scatters charges into the band, with the ultimate result that an equilibrium is quickly established in the impurity system.

We must stress that at a fixed value of V_g, at which the sum of the densities of charges in the 2*D* channel (n_S) and in the depletion layer (n_d) is constant by virtue of electrical neutrality ($n_S + n_d = \text{const}$), the relation between n_S and n_d can be changed markedly by applying an external agent: a) a voltage V_{SB} to the substrate (between the 2*D* channel and the substrate), b) illumination in the far-IR part of the spectrum with a photon energy close to the ionization energy of the impurity ($\hbar\omega \geqslant \Delta_A \approx 50$ meV), or c) illumination in the near-IR region with a photon energy greater than the silicon band gap ($\hbar\omega \geqslant E_g \approx 1$ eV). These are the external agents which we will discuss here, since they are the agents which were used, separately or in combination, in the experiments.

(a) Voltage on the substrate

When a negative voltage V_{SB} is applied between the 2*D* channel and the substrate, the band curvature $e\varphi_D = E_g - eV_{SB}$ (Fig. 1a) extends over the region L_D (the thickness of the depletion layer), so that the surface charge density in the depletion region is $en_d = eN_A L_D$. The charge en_d screens the electric field $\mathscr{E} = \varphi_D/L_D$; we then easily find[1]

$$L_D = \left(\frac{2\varepsilon\varepsilon_0\varphi_D}{eN_A}\right)^{1/2} = \left[\frac{2\varepsilon\varepsilon_0}{eN_A}\left(\frac{E_g}{e} - V_{SB}\right)\right]^{1/2}, \quad (1)$$

$$n_d = \left[\frac{2\varepsilon\varepsilon_0 N_A}{e}\left(\frac{E_g}{e} - V_{SB}\right)\right]^{1/2}, \quad (2)$$

where ε is the dielectric constant of silicon, and ε_0 is the permittivity of free space. Since, for a fixed value of V_g on the metal gate, the charge density en_M is fixed (the capacitance is constant and is determined by the thickness of the insulator, d), we find from the condition of electric neutrality

$$n_M = n_S + n_d. \quad (3)$$

Accordingly, if we hold $V_g = \text{const}$ and determine (from, for example, the Shubnikov–de Haas oscillations) the change in n_S or in the threshold voltage V_T [which is unambiguously related to $n_S = \varepsilon\varepsilon_0(V_g - V_T/ed)$], we can determine the change in the density n_d resulting from variationin V_{SB}.

According to (2), the imposition of a negative voltage V_{SB} and $V_g = \text{const}$ leads to an increase in n_d and therefore a decrease in n_S. The situation is illustrated clearly by Fig. 2, b and c, which shows the magnetoconductivity σ_{xx} as a function of V_g for $H = 7$ T at $V_{SB} = 0$ V and $V_{SB} = -10$ V. The pattern of Shubnikov oscillations shifts as a whole up the V_g scale; this shift corresponds to an increase in the threshold voltage, V_T, as shown in this figure. This shift implies a de-

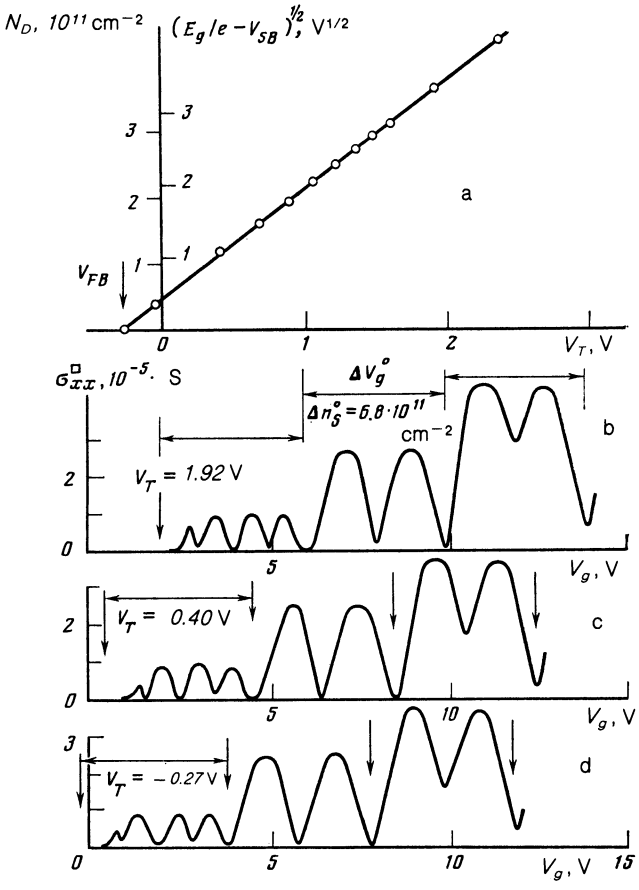

FIG. 2. a—Behavior of the threshold voltage V_T during a variation of the voltage V_{SB}, show as a plot of V_T versus $(E_g/e - V_{SB})^{1/2} \sim n_d$ [see (2)]. The slope of the line is used to determine the quantity $N_A = (7.05 \pm 0.05) \cdot 10^{14}$ cm^{-3}, while the $n_d = 0$ intercept is used to determine the flat-band voltage $V_{FB} = -(0.275 \pm 0.002)$ V; b, c, d—Shubnikov–de Haas oscillations of the magnetoconductivity σ_{xx} versus the gate voltage V_g according to measurements at $H = 7$ T, $T = 1.6$ K, and various values of V_{SB} [b) -10 V; c, d) 0 V]; d—the same, during generation of e-h pairs with a power density $W = -10^{-3}$ W/cm^2. The arrows correspond to complete filling of the Landau levels. The arrow at the extreme left shows the threshold voltage V_T. The quantities ΔV_g^0 and Δn_S^0 are the periods of the oscillations along the voltage and density scales.

crease in n_S at a fixed V_g. Figure 2a shows V_T as a function of $(E_g/e - V_{SB})^{1/2}$ [according to (2) we have $(E_g/e - V_{SB})^{1/2} \sim n_d$], so we have plotted these quantities along a common axis], as found from the shift of the pattern of Shubnikov oscillations in the conductivity at $H = 7$ T and T = 1.6 K. This dependence can be used as a calibration for determining the status of the depletion layer and the charge density en_d in it, from the magnitude of the threshold voltage. Furthermore, the curve of $V_T(V_{SB})$ yields two important parameters: 1) the concentration of acceptors in the substrate, which can easily be determined from the slope of the line, as we see from (2), and 2) the flat-band voltage V_{FB}, i.e., that gate voltage at which there is no band curvature and we have $n_d = 0$ (Fig. 1c). We wish to emphasize that since these results were obtained at low temperatures we used IR illumination with $\hbar\omega \approx 200$ meV to quickly put the impurity system in an equilibrium state.

(b) Effect of radiation which ionizes shallow impurities

As a source of light in the far-IR part of the spectrum we use the intrinsic thermal radiation from the windows of the optical cryostat, which are covered with metal diaphragms which block external light. These windows are at room temperature, so that they emit with a maximum power density at $\hbar\omega \approx 70$ meV. This radiation is sufficient for the establishment of an equilibrium in the impurity system in a time ~ 10 s. Figure 3 shows the behavior of the density of $2D$ electrons, measured at $V_g = 8.4$ V, after a voltage $V_{SB} = -10$ V is applied between the channel and the substrate. In case a there is thermal radiation from the cryostat windows. In case b there is no illumination; the sample is completely covered by a metal screen immersed in the helium. In the former case an equilibrium is completely established in the impurity system (n_d increases and n_S decreases) in a time ~ 100 s, while in the latter case no significant changes in n_S are observed for ordinarily an hour. This circumstance is used to advantage in studying the kinetics of $2D$ electrons with nonequilibrium holes (§8).

(c) Effect of radiation which generates nonequilibrium pairs

We use two sources of light with photon energies greater than the band gap of silicon: an argon laser with $\lambda = 4880$ Å (in the case in which the excitation is carried out through the cryostat windows, and thermal radiation is simultaneously emitted from the outer windows) and a GaAs light-emitting diode, which is placed directly beside the sample in the helium (if it is necessary to block the effects of thermal radiation with $\hbar\omega \approx 200$ meV from the warm windows of the cryostat).

Figure 2d shows the pattern of Shubnikov oscillations of the magnetoconductivity $\sigma_{xx}(V_g)$ during illumination with an argon laser with a power density $W = 10^{-2}$ W/cm^2 at $H = 7$ T, $V_{SB} = 0$ V, and $T = 1.6$ K. We see that the magnetotransport properties of the $2D$ channel do not change substantially when the visible light is turned on (in particular, there is no substantial heating of the system of $2D$ electrons), but the entire pattern of oscillations shifts down the V_g scale, implying a decrease in the threshold voltage. As we mentioned in Subsection 3a, we can use the value of V_T to determine n_d. Using the calibration curve in Fig. 2a, we easily find that during illumination with an argon laser with $W = 10^{-2}$ the threshold voltage is essentially equal to the flat-band voltage. It follows that we have $n_d \approx 0$, and the entire electric field is concentrated in the $2D$ channel; outside this channel, the field is essentially zero (Fig. 1c). We concluded in Ref. 2 that the relation $n_d < 0$ holds during illumination from that conclusion we drew the further con-

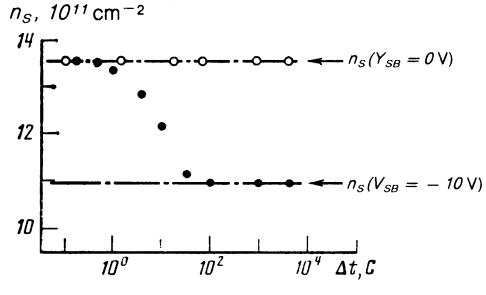

FIG. 3. Changes in the density of $2D$ electrons measured after the application of a voltage $V_{SB} = -10$ V to the substrate (at the time $\Delta t = 0$) with $V_g = 8.40$ V and $T = 1.6$ K. Filled circles—during illumination in the far-IR part of the spectrum, with $\hbar\omega \approx 200$ meV; open circles—in the absence of illumination.

clusion that a second hold layer exists. The possible existence of such a layer during nonequilibrium *e-h* excitation was originally pointed out by Altuhkov *et al.*[4] A more accurate analysis based on a comparison of the voltages V_{FB} and V_T during excitation shows that n_d is positive and less than $n_d \leqslant 10^9$ cm^{-2} (this value corresponds to an electric field $\mathscr{E} \leqslant 10^2$ W/cm in the semiconductor directly beyond the 2*D* channel). Most of the error in our earlier estimates consisted of the error in the determination of N_A, which had previously been found not from the calibration curve $V_T(V_{SB})$ but from the magnitude of the conductivity of a silicon wafer at room temperature. The primary conclusion of this section of the paper is that during generation of *e-h* pairs in the interior of the semiconductor there is essentially no depletion layer, and the electric field in the interior of the semiconductor just beyond the 2*D* channel is weak $\mathscr{E} \leqslant 10^2$ W/cm).

§4. RECOMBINATION RADIATION OF 2*D* ELECTRONS DURING RECOMBINATION WITH INJECTED HOLES

As was established in the preceding section, the depletion layer essentially disappears during nonequilibrium excitation, so that there are neutral acceptors containing holes just beyond the 2*D* channel. Since the wave function of the 2*D* electrons extends into the interior of the semiconductor along the direction $Z \parallel [001]$ $[\psi(Z) \sim Z \exp(-\frac{1}{2}bZ)$, where $b^{-1} \approx 7$–10 Å], there is a nonvanishing probability for the recombination of 2*D* electrons with injected holes. Since this recombination is indirect, however, in both momentum space and coordinate space, we would expect its intensity to be exceedingly weak in comparison with the bulk radiation. It is this faint recombination which is observed experimentally. Figure 4 shows emission spectra recorded at a power density $W \approx 10^{-3}$ W/cm^2 for various gate voltages, corresponding to the densities n_S of 2*D* electrons determined from the Shubnikov oscillations under the same conditions. We see that for $V_g \leqslant V_T$ (i.e., at $n_S = 0$) the recombination spectrum contains only an intense bulk emission line of excitons bound to boron (*BE*). With a further increase in the pump level ($W > 10^{-2}$ W/cm^2), the emission lines of multiexciton-impurity complexes appear,[5] as do emission lines of an electron-hole liquid[6] (at $W > 10$ W/cm^2). The spectral positions of these lines fall in the part of the spectrum in which we are interested here, so that we were forced in practice to work at $W < 10^{-2}$ W/cm. For $V_g > V_T$, at which the 2*D* channel arises, a new line, the $2D_e$ line, appears in the spectrum of the recombination emission. This line has several characteristic properties:

1) The intensity of the emission in the $2D_e$ line is extremely low: two or three orders of magnitude lower than the intensities of the bulk lines.

2) The shape of the $2D_e$ line at high densities n_S, at which a metallic conductivity is observed in the system of 2*D* electrons, is reminiscent of a step function of the energy, reflecting the constancy of the state density of 2*D* electrons.

3) The width of the $2D_e$ line increases linearly with increasing density n_S, in accordance with the change in the Fermi energy of the 2*D* electrons.

4) The spectral position of the violet edge of the $2D_e$ line is essentially independent of V_g (to within an error ≈ 0.5 meV). This property corresponds to a fixed value of the chemical potential of the 2*D* electrons, χ_e (Fig. 1), which is determined by the volume.

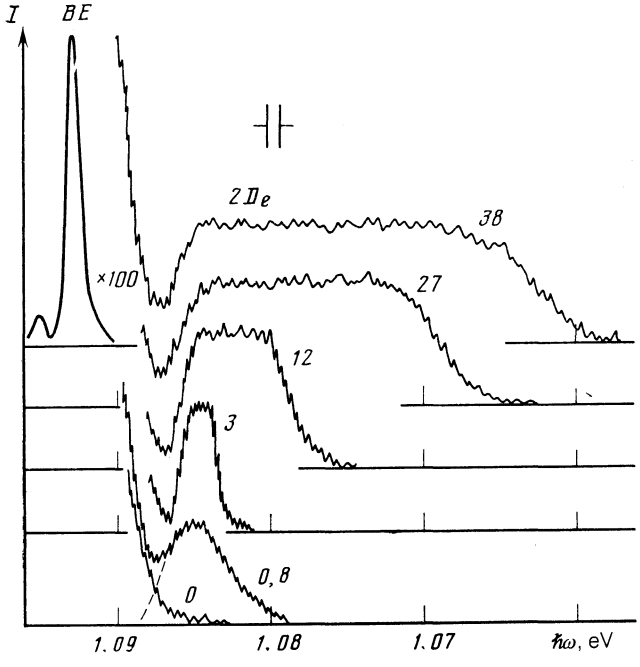

FIG. 4. The *TO*-phonon components of the emission spectrum measured in silicon MIS structure at $T = 1.6$ K, at a power density $W = 10^{-3}$ W/cm^2, and for various positive gate voltages V_g under conditions such that a 2*D* electron channel forms. The density of the 2*D* electrons, n_S, is measured simultaneously, on the basis of the oscillations in the magnetoconductivity. The density values are shown beside the spectra, expressed in units of 10^{11} cm^{-2}. The line *BE* is the emission of excitons bound to boron; the $2D_e$ line corresponds to the radiative recombination of 2*D* electrons.

(a) The $2D_e$ line in the *TO*- and *TA*-phonon and no-phonon components of the spectrum

In order to determine the recombination mechanism we need to first determine with which holes the 2*D* electrons recombine, free holes or holes bound to boron atoms. Intuitively we would expect that recombination with bound holes would be more probable, since their density is substantially higher than that of free holes and, furthermore, they are less affected by the residual electric field which repels free holes away from the 2*D* channel toward the substrate. Perhaps a decisive argument in favor of this assumption is the fact that the corresponding recombination of photoexcited electrons with 2*D* holes produced in the same structures at negative voltage V_g is less intense by at least an order of magnitude.

If holes bound to boron atoms are participating in the recombination, it would be possible to observe a no-phonon emission line shifted up the energy scale, since the momentum carried off by phonon in this case, which is close to the Brillouin momentum, can be transferred to an impurity center.[5] Figure 5 shows the *TO*-phonon, *TA*-phonon, and no-phonon components of the spectrum. We see that in addition to the emission of excitons bound to boron all three components contain the $2D_e$ line, which appears for $V_g > V_T$. In the no-phonon component the emission intensity is so low that the spectrum of the $2D_e$ line was recorded point by point at several fixed energies. It should also be noted that the no-phonon component contains, in addition to emission from the volume of excitons bound to boron [the *BE*(*B*) line], emission of comparable intensity from excitons bound to

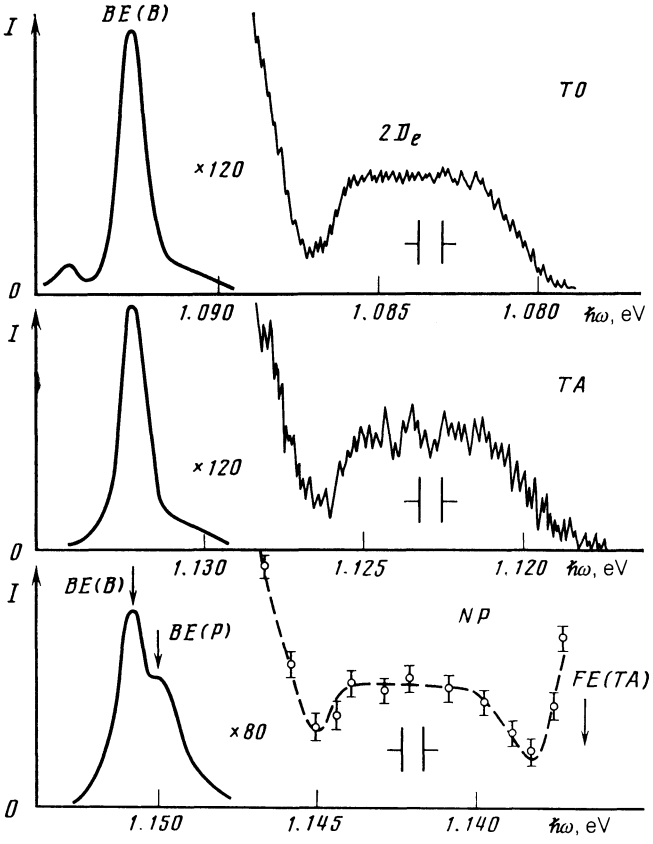

FIG. 5. The *TO*- and *TA*-phonon components and the no-phonon component of the emission spectrum found at $W = 10^{-3}$ W·cm^2, $T = 1.6$ K and $n_S = 9\cdot 19^{11}$ cm^{-2}. The lines $BE(B)$ and $BE(P)$ are emission of excitons bound with boron and phosphorous atoms, respectively; the $2D_e$ line corresponds to the radiative recombination of $2D$ electrons.

phosphorus [the $BE(P)$ line]. The phosphorus concentration in the silicon substrate is two orders of magnitude lower than the boron concentration. The reason is that the probability for a no-phonon recombination of excitons bound to boron atoms is nearly three orders of magnitude lower than for phosphorus.[5]

(b) Violet boundary of the $2D_e$ line

It can be seen from Fig. 4 that a characteristic feature of the $2D_e$ line is the independence of the violet boundary of the line from the gate voltage V_g (or from the density n_S). This experimental fact can be explained easily in terms of a radiative transition from fixed-energy levels of the chemical potentials of electrons and holes, which are determined by the volume and which essentially coincide with the bottoms of the corresponding bands during nonequilibrium excitation at low temperatures. As was established above, however, the recombination of the $2D$ electrons occurs with holes bound to boron; i.e., it corresponds to a transition from the conduction band to an impurity level which lies a distance from the bottom of the valence band equal to the ionization energy of the acceptor, $\Delta_A = 46$ meV.

We would thus expect that the violet boundary of the $2D_e$ line would lie a distance $\Delta\hbar\omega$, close to Δ_A, from the edge of the band gap. Experimentally, however, we find $\Delta\hbar\omega = 25$ meV. This fact means that not all of the binding energy of the hole at the acceptor—only part of it—is taken as a result of the recombination. The implication is that a bound complex with a binding energy ≈ 20 meV remains in the final state. Indeed, a negatively charged boron atom remains as a result of recombination in the impurity system; in addition, there is a positively charged excitation: a hole in the Fermi sea of $2D$ electrons. These charges may form a bound complex with a binding energy ≈ 20 meV. An important point is that this complex of a negatively charged impurity and a quasi-$2D$ hole should have typical values of the Bohr radius a^* and the energy $\mathrm{Ry}^* = e^2/2\varepsilon a^*$, since the broadening due to the holes is slight (≈ 0.5 meV; Ref. 3). Estimates yield $\mathrm{Ry}^* \approx 20$ meV; we then find $a^* = 60$ Å. This value agrees reasonably well with the thickness of the $2D$ electron channel.

The process by which $2D$ electrons recombine with injected holes can thus be represented as follows. Essentially the entire electric field in the semiconductor and the $2D$ electrons are concentrated in a very narrow region near the interface. In this region, the boron atoms are fully ionized, and the hole density is zero. The electric field decreases rapidly with distance from the interface into the interior, reaching a level $\sim 10^2$ V/cm at a distance ~ 70 Å. It is at this distance where neutral acceptors appear. The density of $2D$ electrons reaches a maximum at $Z = 3b^{-1} \approx 20$ Å. The wave function of these electrons, however, stretches into the interior of the semiconductor, and the overlap integral of the electron and hole wave functions—this integral determines the recombination probability—reaches a maximum at $Z = Z_0$ and falls off sharply on both sides, in an interval ΔZ. Consequently, only holes from a thin layer with a $2D$ density $n_h \approx 10^9$ cm^{-2} are effective in recombination (see §8 for more details on the measurement of ΔZ and n_h). As a result of the recombination, a hole bound to a boron atom is essentially converted into a positively charged excitation, a hole in the $2D$ channel. It follows from energy conservation that the energy deficit ΔE_x is equal to the difference between the binding energies of these two complexes. From the experiments we find $\Delta E_x = 20$ meV.

(c) Shape of the $2D_e$ line

The lineshape of the emission of $2D$ electrons as they recombine with nonequilibrium holes in a process involving a *TO* phonon (here we have a matrix element $M_{TO} = \mathrm{const}$) is described by the convolution of the electron and hole distribution functions[6]:

$$I(\hbar\omega) \sim \int_0^\infty F_e(E) F_h(\hbar\omega - E)\, dE, \tag{4}$$

$$F_{e(h)} = f_{e(h)} D_{e(h)}, \tag{5}$$

where $f_{e(h)}$ and $D_{e(h)}$ are the distribution function and state density of the electrons (holes). It follows from (4) that the functions F_e and F_h can be determined separately if we make one of them, say the electron function, very narrow in comparison with the other. If we do this, we can treat this function as a Dirac δ-function, so that the shape of the emission line will directly reflect F_h. The distribution function of the $2D$ electrons in a strong magnetic field perpendicular to the $2D$ layer is approximately a δ-function when the Landau level is half full.[1,7] In this case, as follows from our experiments, the width of F_e is less than ≈ 3 K in the highest-quality structures.[3] The emission spectrum found under

these experimental conditions is approximately triangular with a half-width ≈ 10 K which is independent of μ, H, and the size of the spectral gap. This function could naturally be regarded as the hole distribution function $F_h(E)$. Fortunately, $F_h(E)$ also turns out to be narrow in comparison with the characteristic Fermi energy of the $2D$ electrons (e.g., $E_F \approx 70$ K at $n_S = 10^{12}$ cm^{-2}). This result means that the spectrum of the recombination of $2D$ electrons with nonequilibrium holes is the function $F_e(E)$. Since both functions $f_e(E)$ and $D_e(E)$ are essentially θ-functions in the absence of a magnetic field and at low tempertures, the emission spectrum should be a step function of the energy of width E_F. The measured $2D_e$ lineshape is indeed close to that expected, but at low energies we see a significant smearing of r instead of a sharp edge near the bottom of the quantum-size band E_0 (Fig. 4). The absolute value of this smearing increases with increasing density n_S. The latter circumstance is evidence that this deviation from the expected shape is a consequence of the attenuation of one-electron excitations in the Fermi sea of $2D$ electrons.

The system of $2D$ electrons is an example of a Fermi liquid whose properties can be described in terms of noninteracting one-particle excitations characterized by a distinctive dispersion law and an attenuation Γ. Theoretical predictions[1,8] show that the interaction of $2D$ electrons leads to some renormalization of the mass of the excitations in comparison with the mass of noninteracting electrons (§5). The magnitude of the attenuation of the excitations can be determined theoretically only near the Fermi surface. It can be asserted, however,[9] that if Γ is zero at the Fermi surface, increases with distance from E_F, and reaches a maximum at the two bands with $E = E_0$. Consequently, it is at the red edge of the $2D_e$ line, which corresponds to transitions from the bottom of the band, that the effects of Fermi attenuation will be seen most clearly, in agreement with experiment. As the density n_S is increased, the electron-electron interaction intensifies, and Γ increases as a result. The presence of intense bulk emission (the BE line) at the violet edge and the manifestation of attenuation effects at the red edge of the $2D_e$ line complicate a direct determination of the position of the level, E_0, and the Fermi energy E_F. Instead of going through the procedure of approximating the shape of the $2D_e$ line with adjustable parameters E_F and Γ, we can find the Fermi energy of the $2D$ electrons and the attenuation at the bottom of the band through a study of the pattern of the Landau levels in a magnetic field. Without going into detail on the features of the state density of $2D$ electrons in a perpendicular magnetic field (which will be the subject of a separate paper), we note that N lines are observed in the emission spectrum when N Landau levels are completely filled, i.e., at $n_S = 4NeH/h$ (Ref. 3). Figure 6 shows emission spectra obtained at $n_S = 2.7 \cdot 10^{12}$ cm^{-2} and $H = 7$ T, with $N = 4$ (the filling factor is $\nu = 16$ because of the fourfold degeneracy of the levels in spin and valley). With decreasing magnetic field, the pattern of Landau levels becomes more congested, and we observe the fan shown at the upper part of this figure. It is easy to see that the extreme points to which the Landau levels converge in the limit $H\,O$ directly determine the positions of E_0 and E_F in the emission spectrum. The smearing at the red edge of the $2D_e$ line corresponds to the maximum attenuation, i.e., to the value of Γ at the bottom of the band. Analysis of the spectra by this method reveals that (1) the Fermi energy of the $2D$ electrons increases linearly with increasing n_S (§6), in accordance with a constant state density in a zero magnetic field, (2) the state-density mass found from the curve of $E_F(n_S)$ is $m_d = (0.202 \pm 0.002)m_0$ (m_0 is the mass of a free electron), or just slightly greater than the mass of noninteracting electrons, $0.19m_0$, and (3) the cyclotron mass found from the fan of the splitting between Landau levels (Fig. 6) is $m_c = (0.200 \pm 0.003)m_0$.

§5. POLARIZATION OF THE $2D_E$ LINE

In a cubic silicon crystal, the symmetry makes all directions equivalent, and the recombination radiation will be upolarized if there are no external agents. If a uniaxial deformation or magnetic field is imposed, the symmetry is reduced and the emission becomes polarized. In the case of the recombination of $2D$ electrons with nonequilibrium holes, there is a preferred direction in the system normal to the $2D$ layer. That this is a preferred direction can be seen in the circumstance that the quantization of the motion along the

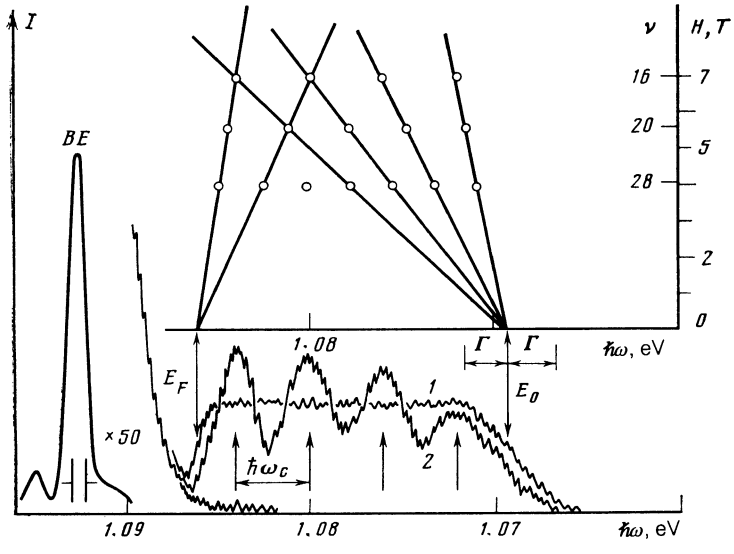

FIG. 6. Spectra of the recombination radiation of $2D$ electrons recorded at $T = 1.6$ K, $W = 10^{-3}$ W/cm^2, and $n_S = 2.7 \cdot 10^{12}$ cm^{-2} in a perpendicular magnetic field $H = 7$ T (spectrum 2; four Landau levels are completely filled) or at $H = 0$ (spectrum 1). The arrows show the positions of the four Landau levels in the spectrum. The points in the upper part of this figure show the energy positions of the Landau levels in magnetic fields of 7, 5.6, and 4 T, at which respectively four, five, and seven levels are completely filled at $n_S = 2.7 \cdot 10^{11}$ cm^{-2}. The extreme points in the splitting fan determines the positions of the Fermi energy E_F and the band bottom E_0; Γ is the smearing of the red edge of the $2D_e$ line due to the attenuation of one-particle excitations.

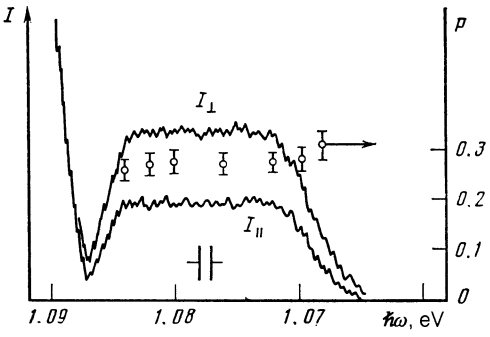

FIG. 7. Spectra of the recombination radiation of 2D electrons (the TO-phonon component) measured in two polarizations; along ($I_\parallel$) and across ($I_\perp$) the normal to the 2D electron layer, for $n_S = 2.7\cdot 10^{12}$ cm^{-2} and $T = 1.6$ K ($H = 0$). Also shown here is the degree of linear polarization, $P = (I_\perp - I_\parallel)/(I_\perp + I_\parallel)$.

Z direction only two electron valleys (of the six), which lie on the [001] axis, are populated; for them, the mass in the Z direction is maximal. It is thus clear that in such a system we should expect linearly polarized recombination radiation. Figure 7 shows emission spectra obtained in two polarizations: $I_\perp$, i.e., with the vector E perpendicular to the [001] axis and lying in the 2D plane, and $I_\parallel$ i.e., with the vector E directed parallel to the normal to the 2D layer.

The entire emission spectrum is seen to be uniformly (in energy) linearly polarized in the 2D plane, and the degree of polarization is $P = (I_\perp - I_\parallel)/I_\perp + I_\parallel) \approx 0.28$. The absolute value of P was found by allowing for the depolarization coefficient of the optical system, $\gamma \approx 0.75$, which was determined by special measurements of the degree of polarization of well-known bulk emission lines in a magnetic field. The degee of linear polarization should be compared with the theoretical prediction and also with the results of corresponding experiments carried out with uniformly deformed silicon crystals. During compression and extension of silicon along the (001) axis, one observes a polarized emission of excitons consisting of electrons belonging to only two (001) valleys with holes with $J_Z = 1/2$ (compression) or $J_Z = 3/2$ (extension). Theoretical and experimental results for these cases were published in Refs. 5, 10, and 11. Table I shows the selection rules for optical transitions involving electrons belonging to (001) valleys and holes with different projections J_Z. This table shows absolute values found[5] for $\alpha = (1/2)\beta$, in which case we find the best agreement between the theoretical values and the experimental values from experiments with deformed silicon.[10] It can be seen from this table that if the state of the holes which combine with the 2D electrons were a doublet with $J_Z = 1/2$ or $J_Z = 3/2$, the $2D_e$ line would have a polarization of the other sign ($J_Z = 1/2$) or would have a very high degree of polarization (if $J_Z = 3/2$). If we assume that all the projections of the total angular momentum of the holes, $J_Z = 3/2$, are participating in the recombination, then the theoretical values for the degree of polarization would come very close to that found experimentally (Table I).

We found the same sign of the polarization and the same degree of polarization for the $2D_e$ line in the TA-phonon component of the spectrum. This result is not unexpected, since the selection rules are the same for transitions involving TO and TA phonons.

§6. SCREENING OF THE RANDOM POTENTIAL OF DEFECTS

To determine the Fermi energy accurately from the shape of the $2D_e$ line, we can use the linewidth measured at half-maximum, ΔE (§4). Figure 8 shows ΔE as a function of the density n_S according to measurements with two structures with maximum 2D-electron mobilities of $1.7\cdot 10^4$ cm^2/(V·s) and $3.1\cdot 10^4$ cm^2/(V·s). We see from this figure that for $n_S > 3\cdot 10^{11}$ cm^{-2}, up to $n_S = 4\cdot 10^{12}$ cm^{-2}, there is a strictly linear functional dependence $\Delta E(n_S)$, which reflects the fact that the state density of the 2D electrons is constant,

$$D_e = 2m_d/\pi\hbar^2 = \text{const}, \qquad (P)$$

and the relation $E_F = n_S/D_e$ holds. For densities $n_S < 3\cdot 10^{11}$ cm^{-2} we observe a nonmonotonic functional dependence $\Delta E(n_S)$. The lower part of Fig. 8 shows the degree of linear polarization, P, of the $2D_e$ line as function of the density n_S. We see that P as constant and independent of n_S for $n_S > 3\cdot 10^{11}$ cm^{-2}, while for $n_S < 3\cdot 10^{11}$ cm^{-2} it decays to zero as n_S decreases.

To determine the reasons for these features it is interesting to compare the results found for two samples differing in quality, differing in the maximum mobility of the 2D electrons, and differing in the density of localized states. The difference in the density of localized states is seen in the fact that, for example, the metallic conductivity arises in the 2D channel at different critical densities n_S^0. The value of n_S^0 is found by extrapolating the n_S dependence of the activation energy W to $W \to 0$; it is shown by the arrows for the two structures.[12] For $n_S < n_S^0$ it is metallic. It can be seen from Fig. 8 that in the structure with the smaller value of n_S^0 the contraction of the $2D_e$ line and the appearance of a polarization are observed at lower values of n_S. This result is evidence that these phenomena are caused by screening of the random potential of defects at the semiconductor-insulator interface.

At low values of n_S ($n_S < n_S^0$) and at low temperatures ($T < W$), the 2D electrons are highly localized at fluctuations of the random potential, and the conductivity has a thermal-activation nature in this case. When localization is pronounced, the relaxation of 2D electrons from high-energy to low-energy states occurs very slowly in comparison

TABLE I

Electron valley	J_Z	$I_\parallel$	$I_\perp$	$P = (I_\perp - I_\parallel)/(I_\perp + I_\parallel)$
(001)	$1/2$	α^2	$2\beta^2$	0.78 (theor)
(001)	$3/2$	$3\alpha^2$	0	− 1.00 (theor)
(001)	$3/2$, $1/2$	$4\alpha^2$	$2\beta^2$	0.33 (theor)
				0.28 (expt)

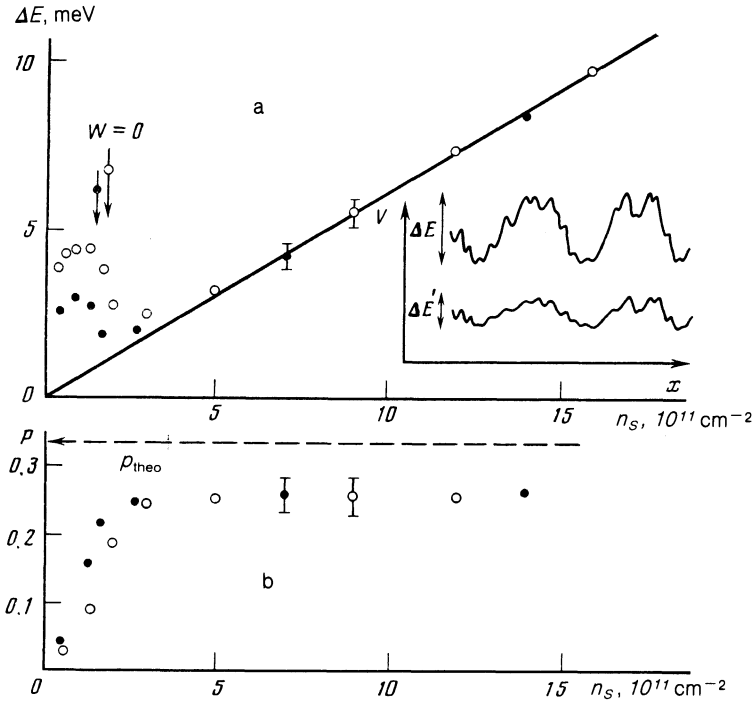

FIG. 8. a—Half-width of the $2D_e$ line; b—degree of linear polarization, P, versus the density of $2D$ electrons, n_S, found at $T = 1.6$ K for two metal-insulator-semiconductor structures with a maximum $2D$-electron mobility of $3\cdot10^4$ cm^2/(V·s) (filled circles) or $1.7\cdot10^4$ cm^2/(V·s) (open circles). The arrows show the density n_S^0, at which the insulator-metal transition occurs in the $2D$ system. The inset is a schematic plot of the variation in the random potential of defects along the Si–SiO_2 interface and in the linewidth ΔE as n_S increases.

with recombination, so that at a quasiequilibrium we may assume that all the states are filled nearly uniformly, regardless of their energy. It is for this reason that for $n_S < n_S^0$ we observe a broad $2D_e$ line, for which ΔE apparently corresponds to the amplitude of the fluctuations in the random potential of defects at the interface (§7). As n_S increases, the localized states become filled, and at n_S^0 the $2D$ electrons become delocalized. As a result, the screening of the random potential becomes effective (see the inset in Fig. 8), and the recombination line becomes significantly narrower. Its subsequent broadening reflects an increase in the Fermi energy of the $2D$ electrons with increasing density n_S.

It is interesting to examine the behavior of the linear polarization of the $2D_e$ line as a function of the density n_S. At $n_S < n_S^0$ (the metallic region) the degree of polarization is constant over the entire width of the $2D_e$ line (Fig. 7) and does not depend on the density of $2D$ electrons. At $n_S < n_S^0$ (the region of strong localization), the degree of linear polarization decreases with increasing n_S. This result can be understood easily by noting that the random potential of the defects mixes the localized states of the electrons over all six valleys. For electrons which are more strongly bound, this mixing is more pronounced, and the degree of polarization of the emission is ultimately lower. There is no such mixing in the metallic region, and the $2D$ electrons belong to only two valleys in the (001) axis, so that the degree of polarization of the $2D_e$ line is maximized. We thus find a spectroscopic method for preparing the region of strong localization from the region of metallic conductivity, by examining the n_S dependence of the degree of polarization.

§ 7. DETERMINATION OF THE ABSOLUTE VALUE OF THE STATE DENSITY AND OF THE OCCUPATION NUMBERS WHEN THE 2D ELECTRONS ARE HIGHLY LOCALIZED

As was mentioned back in §4, the emission spectrum of the $2D$ electrons, $I(E)$, is the product of the functions $f_e(E)$ and $D_e(E)$, where the origin for the E scale is at the bottom of the band, EO. Since the density is related to f_e and D_e by

$$n_S = \int_0^\infty f_e(E) D_e(E)\, dE, \tag{6}$$

the integrated emission intensity is constant at a fixed n_S. We can make use of this fact to determine the absolute value of the state density of the $2D$ electrons under any experimental conditions, by making a comparison with the emission spectrum in a zero magnetic field. Specifically, since we know that the state density of the $2D$ electrons is constant at $H = 0$ and given by $D_0 = 2m_d/\pi\hbar^2 = 1.7\times10^{11}$ cm^{-2} ·meV^{-1} (§4), we can use the known positions of E_0 and E_F and the equality of the areas in the rectangle in Fig. 9a and under the $2D_e$ emission line to find the value of D_0 on the intensity scale (Fig. 9a). After carrying out this procedure, we can determine (for example) how the absolute value of the state density changes in a perpendicular magnetic field (at n_S = const), by equating the spectral intensities of the $2D_e$ emission lines at $H = 0$ and $H \neq 0$ (Ref. 3). We should stress that this procedure is legitimate only if the occupation numbers are unity, i.e., first, at $H = 0$ and $E_F \gg T$ and, second, when the Landau levels are completely filled with $H \neq 0$.

When the $2D$ electrons are highly localized [at small values of n_S ($n_S \ll n_S^0$) or when the quantum Hall is present with $H \neq 0$, Refs. 13 and 14] the electron system may not reach equilibrium during the recombination time (§6), and the occupation numbers may be different from unity. Methods of optical spectroscopy can be used in this case to determine the occupation numbers when the electrons are highly localized if the function $D_e(E)$ is known. To measure the energy distribution of the state density of $2D$ electrons under strong localization conditions, one can measure the thermal-activation conductivity.[12] The idea of this method is that as the localized states are filled the Fermi quasilevel of the $2D$ electrons approaches the mobility threshold, an the activation energy W decreases. One can thus employ the functional

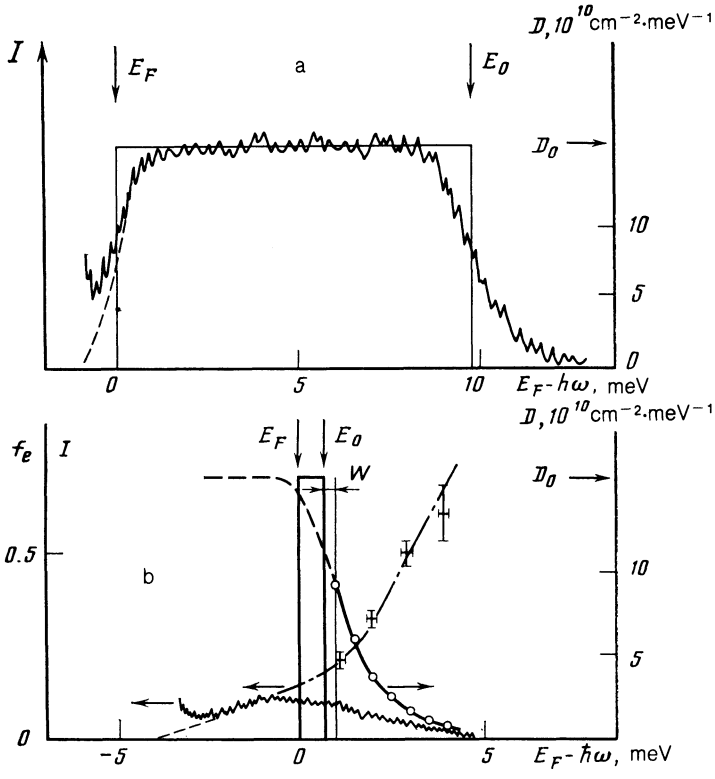

FIG. 9. a—Determination of the absolute value of the state density D of the $2D$ electrons at $n_S = 1.6 \cdot 10^{12}$ cm^{-2}; b—determination of the occupation numbers f under conditions of strong localization with $n_S = 1.2 \cdot 10^{11}$ cm^{-2}, from the recombination-radiation spectra (see the text proper for an explanation).

dependence $W(n_S)$ to find the function $D_e(E)$ by differentiation. We should stress that this procedure presupposes that the function $D_e(E)$ depends strongly on n_S, because of screening of the random defect potential at the Si-SiO$_2$ interface. Nevertheless, there is a range of n_S values (Fig. 8) in which the screening effects have not yet become important, and the procedure of determining $D_e(E)$ from the thermal-activation conductivity is legitimate. Figure 9b shows the functional dependence $D_e(E)$ found by this method. We should point out that this dependence was measured in the absence of nonequilibrium excitation and with $n_d = 0$. The reasons are that (first) only under these conditions are the occupation numbers f_e approximately unity and (second) during illumination the bulk photoconductivity is comparable in magnitude to the conductivity of this system of highly localized $2D$ electrons. The latter circumstance makes it difficult to determine the activation energy of the $2D$ electrons during photoexcitation.

It can be seen from Fig. 9b that the occupation numbers $f_e(E)$ found by comparing $I(E)$ and $D_e(E)$ are substantially less than unity during cw excitation in the region where the $2D$ electrons are highly localized. Here we observe a decrease in $f_e(E)$ with increasing energy E. We also find that with decreasing n_S and thus increasing activation energy W the values found for $f_e(E)$ by this analysis technique become smaller. Furthermore, the localized states associated with fluctuations of the random defect potential are filled more uniformly [i.e., the function $f_e(E)$ becomes independent of the energy: $[f_e(E) \approx f_e^0 = \text{const}]$. Knowing f_e^0 for a given n_S, we can determine the density of localized states at the Si-SiO$_2$ interface: $n_l = n_S/f_e^0$. In a sample with $\mu^* = 1.7 \cdot 10^4$ cm^2/(V·s), this value is found to be $n_l = 2 \cdot 10^{11}$ cm^{-2}.

In summary, the simultaneous use of methods of optical spectroscopy and electron transport makes it possible to determine the absolute value and energy distribution of the state density and of the occupation numbers of the $2D$ electrons.

§8. KINETICS OF THE RECOMBINATION OF 2D ELECTRONS WITH NONEQUILIBRIUM HOLES

The emission in the $2D_e$ line is extremely weak, as we have already mentioned. For this reason we were unable to directly measure the recombination time constant τ_r by examining the kinetics of the emission in the $2D_e$ line. We were nevertheless able to estimate the characteristic time τ_r from the kinetics of the magnetoconductivity, which reflects the time evolution of the density n_S. To illustrate the approach, we consider the case in which the electron-hole pairs are generated with the help of a GaAs light-emitting diode, and the sample, in a cold ($T \approx 2$ K) metal cup, is illuminated exclusively in the near-IR region ($\hbar\omega \geqslant E_g$). Under these conditions, a certain fraction Δn_S of the $2D$ electrons should undergo recombination with close-lying holes from the rather narrow region ΔZ over a characteristic time τ_r after the light is turned off (this can be done in $\sim 10^{-6}$ s). After this recombination, essentially no changes will occur in the $2D$ channel or in the impurity system (§3 and Fig. 3). A study of the kinetics of the density of $2D$ electrons on the basis of the magnetoconductivity thus not only yields an estimate of the characteristic time but also reveals the density of holes which are effectively involved in recombination: $\Delta n_h = \Delta n_S$. Furthermore, the size scale of the region in which the recombination occurs, $\Delta Z = \Delta n_h / N_A$, can be estimated from the kinetics of the magnetoconductivity.

The upper part of Fig. 10 shows how the pattern of Shubnikov oscillations (for the minimum of σ_{xx}, corresponding to $\nu = 4$), shifts as the excitation power is reduced from 10^{-1} W/cm^2 to 0. We see that at $W = 10^{-3}$ W/cm^2 the $2D$ density electron stops changing as the excitation power is

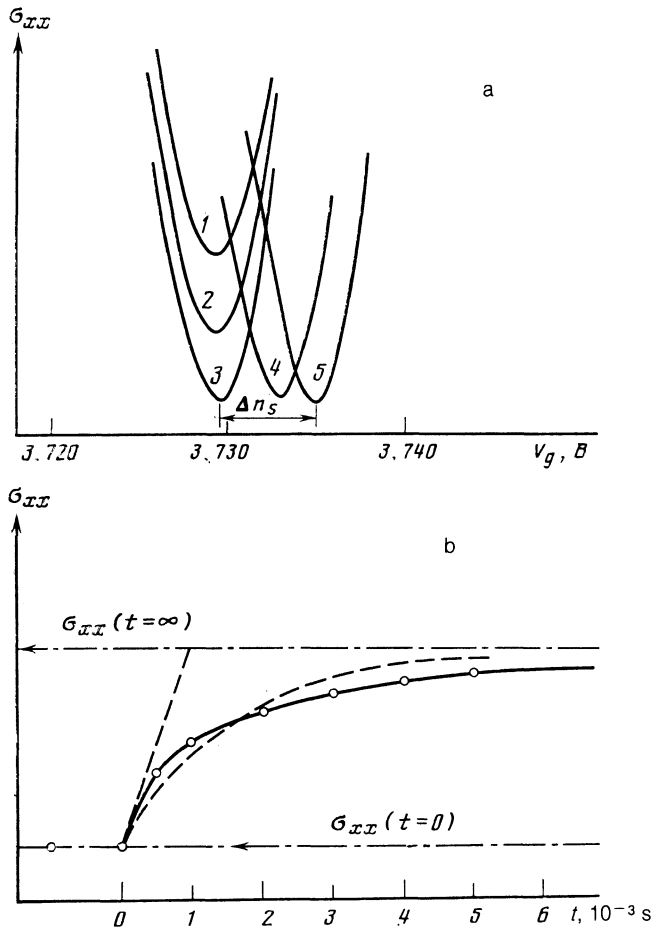

FIG. 10. a: Behavior of the magnetoconductivity σ_{xx} at the minimum corresponding to $\nu = 4$ ($H = 7$ T, $T = 1.6$ K) found during e-h excitation by light with $\hbar\omega = 1.5$ eV for various values of the power density. 1—$W = 10^{-1}$; 2—10^{-2}; 3—10^{-4}; 4—10^{-5}; 5—0 W/cm^2 ($\Delta n_S = 9\cdot 10^8$ cm^{-2}. b: Magnetoconductivity kinetics σ_{xx} measured near the maximum of σ_{xx} ($\nu = 5.5$, $V_g = 5.3$ V, $H = 7$ T, $T = 1.6$ K) after the light with $\hbar\omega = 1.5$ eV is turned off (at $t = 0$). The characteristic time is $\tau_r \approx 10^{-3}$ s.

raised. The increase in the absolute value of σ_{xx} at the minimum $W > 10^{-2}$ W/cm^2 is due to very slight heating of the system of $2D$ electrons (by ≈ 0.1 K at $W = 10^{-1}$ W/cm^2). As the excitation power is reduced, the pattern of Shubnikov oscillations shifts up the V_g scale; this shift corresponds to an increase in V_T and thus a decrease in n_S at a fixed V_g. The change in the density of $2D$ electrons as a reseult of their recombination with nonequilibrium holes is $\Delta n_S = 9\cdot 10^8$ cm^{-2}, as can be seen from Fig. 10. In order to record the changes in n_S, we had to work hard at a maximum of σ_{xx}, e.g., at $\nu = 5.5$, instead of at a minimum, in order to eliminate the effect of the parasitic time $\tau = RC$ (where $R \approx \sigma_{xx}^{-1}$, and C is the capacitance of the MIS structure). At a minimum of σ_{xx}, this time can reach ~ 1 s, while at a maximum of σ_{xx} it is $\sim 10^{-6}$ s. The lower part of Fig. 10 shows the time evolution of the increase in the magnetoconductivity at $\nu = 5.5$ as the result of the decrease in the density of $2D$ electrons after the light is turned off. We first note that the experimental dependence is not exponential (the dashed curve). The reason is that the recombination of the $2D$ electrons occurs with holes at various distances Z_0 from the interface, and the probability for recombination with them (and also the recombination time) varies with Z. Nevertheless, the characteristic time τ_r can be estimated from the slope of the $\sigma_{xx}(t)$ curve (in the limit $t \to 0$) $\approx 10^{-3}$ s. Knowing that the density of $2D$ electrons (and thus that of the holes) decreases by $\Delta n_S = \Delta n_h = 4\cdot 10^8$ cm^{-2}, over the time τ_r, we can estimate the size scale (ΔZ) of the region in which the recombination occurs: $\Delta Z = \Delta n_h / N_A \simeq 40$ Å.

§9. EFFECT OF ATTENUATION AND IMPURITY EFFECTS ON THE SHAPE OF THE $2D_e$ LINE

As we pointed out back in §4, the properties of a system of interacting $2D$ electrons—an example of a Fermi liquid—should be described in terms of noninteracting one-particle excitations. It follows from the studies of the shape of the $2D_e$ line and the behavior of its width and the pattern of splitting of Landau levels in a transverse magnetic field that the state-density mass for the excitations differs only slightly from the mass of noninteracting $2D$ electrons (§4). In our case, nothing can be said at the outset about the magnitude of the attenuation of one-particle excitations, Γ. If we draw upon the analogy with known Fermi-liquid systems, e.g., the electron-hole liquids in Ge and Si, we can say that the attenuation increases with distance from the Fermi surface and reaches a maximum value $\Gamma_{\max}$ at the very bottom of the band. The value of $\Gamma_{\max}$ can range from 10% to 40% of the Fermi energy[15] for various densities of the liquid.

In the system of $2D$ electrons at the silicon (100) surface, the attenuation of one-particle excitations causes a significant spreading of the red edge of the $2D_e$ line, and the value of $\Gamma_{\max}$ at the band bottom is $\Gamma_{\max} = 0.15E_F$ for $n_S = 2.7\cdot 10^{12}$ cm^{-2} (Fig. 6). The magnitude of the attenuation and its variation with distance from the Fermi surface can also be determined from the broadening of Landau levels in the emission spectrum in a transverse magnetic field. It follows from curve 2 in Fig. 6 that the Landau levels split with distance inward from the Fermi surface. At the bottom of the band this broadening is ≈ 2 meV, in agreement with the value found at $H = 0$. It can be seen from Fig. 4 that with increasing n_S the absolute value of $\Gamma_{\max}$ increases and leads to a substantial blurring of the red edge of the $2D_e$ line. The increase in $\Gamma_{\max}$ with n_S is attributed to an enhancement of the effects of the interaction of the $2D$ electrons. The behavior $\Gamma_{\max}(n_S)$ is approximately linear. We find $\Gamma_{\max} = 1.1$ meV at $n_S = 1.2\cdot 10^{12}$ cm^{-2}, $\Gamma_{\max} = 2.0$ meV at $n_S = 2.7\cdot 10^{12}$ cm^{-2}, and $\Gamma_{\max} + 4.0$ meV at $n_S = 3.8\cdot 10^{-12}$ cm^{-2}.

In addition to the attenuation effects, the shape of the $2D_e$ line may be affected by the presence of impurities and imperfections near the Si-SiO$_2$ interface. In fact, the wave function of the $2D$ electrons in the Z direction is, in the ideal case, identical for all the electrons and independent of the energy of the motion of the $2D$ electrons in the plane. However, the presence of defects near the $2D$ channel may lead to a scattering of the $2D$ electrons, with the result that the momentum and energy of the motion in the plane may be transformed into components of the motion along Z. As a consequence of this process, the probability for the tunneling of $2D$ electrons into the interior of the semiconductor increases for the high-energy electrons, with the result that an increase in the emission intensity should be observed at the violet edge of the $2D_e$ line. To see the effects of the scattering by impurities, we studied the shape of the $2D_e$ line in samples differing widely in quality at a constant density of $2D$ elec-

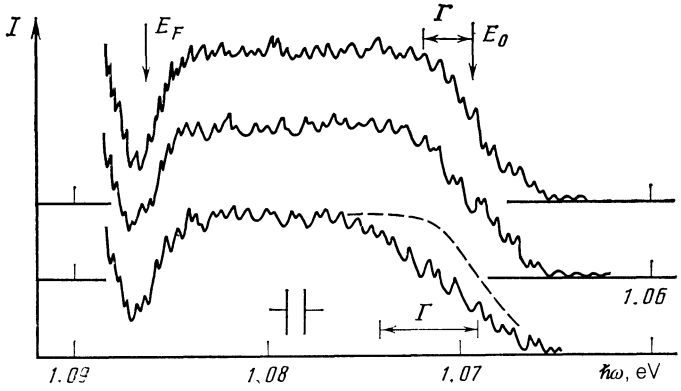

FIG. 11. Comparison of the radiative recombination lines of $2D$ electrons measured under identical conditions ($n_S = 2.7\cdot10^{12}$ cm^{-2}, $W = 10^{-3}$ W/cm^2, $T = 1.6$ K, $H = 0$) from three metal-insulator-semiconductor structures differing in quality. The maximum mobilities of the $2D$ electrons are, from top to bottom, $\mu^* + 3\cdot10^4$, $1.8\cdot10^4$, $4\cdot10^3$ m^2/(V·s).

trons, $n_S = 2.7\cdot10^{12}$ cm^{-2} (Fig. 11). As was mentioned in §2, the structures which we studied differ substantially in both the boron concentration in the substrate (which ranged from $5\cdot10^{14}$ cm^{-3} to $2\cdot10^{15}$ cm^{-3} and the maximum mobility of the $2D$ electrons [μ^* ranged from $4\cdot10^3$ cm^3/(V·s) to $3\cdot10^4$ cm^2/(V·s)]. Of the seven MIS structures, the six with $\mu^* > 10^4$ cm^2/(V·s) had essentially identical shapes of the $2D_e$ line at $n_S = 2.7\cdot10^{12}$ cm^{-2}; only one structure, of the lowest quality, with $\mu^* = 4\cdot10^3$/(V·s), deviated from this shape of the $2D_e$ line, at low energies (Fig. 11). It should be noted that the observed change in the shape of the $2D_e$ line does not agree well at all with the model of an increase in the tunneling probability due to impurity scattering, since it can be seen from the spectra that it is the red, not the violet, edge of the $2D_e$ line which changes. Consequently, the observed deviation in the shape of the $2D_e$ line is probably due to a change in the structure of the state density of the $2D$ electrons in the presence of the random potential of defects with a large fluctuation amplitude.

§10. CONCLUSION

On the basis of these studies of the radiation recombinatin of $2D$ electrons with nonequilibrium holes it can be asserted that the simultaneous use of optical spectroscopy and electron-transport measurements opens up some important opportunities for studying the density of localized and mobile states of $2D$ electrons, phenomena associated with the screening of the random potential of defects, and also Fermi-liquid effects, both with and without a transverse magnetic field. We would particularly like to point out that we pin much hope on the use of optical spectroscopy to study the condensation of a gas of $2D$ electrons into an incompressible Fermi liquid. This event would be seen in the magnetotransport as a fractional quantization of the Hall resistance.[16–18] This new and unusually interesting event has previously been studied only by magnetotransport methods, under conditions such that the interpretation of the results in terms of an activated magnetoconductivity does not always have a solid foundation. Under the circumstances, it is mandatory to appeal to other methods to find information.

We wish to thank S. V. Iordanskiĭ, S. V. Meshkov, E. I. Rashba, and D. E. Khmel'nitskiĭ for useful discussions.

[1)]Since the inner quartz windows of the cryostat transmit only light with $\hbar\omega \geqslant 200$ meV, the maximum of the transmitted thermal radiation turns out to lie at $\hbar\omega \approx 200$ meV.

[1]T. Ando, A. B. Fowler, and F. Stern, Rev. Mod. Phys. **54**, 437 (1982).
[2]I. V. Kukushkin and V. B. Timofeev, Pis'ma Zh. Eksp. Teor. Fiz. **40**, 413 (1984) [JETP Lett. **40**, 1231 (1984)].
[3]I. V. Kukushkin and V. B. Timofeev, Pis'ma Zh. Eksp. Teor. **43**, 387 (1986) [JETP Lett. **43**, 499 (1986)].
[4]P. D. Altukhov, A. V. Ivanov, Yu. N. Lomasov, and A. A. Rogachev, Pis'ma Zh. Eksp. Teor. Fiz. **38**, 5 (1983) [JETP Lett. **38**, 4 (1983)].
[5]V. D. Kulakovskiĭ, G. E. Pikus, and V. B. Timofeev, Usp. Fiz. Nauk **135**, 237 (1981) [Sov. Phys. Usp. **24**, 815 (1981)].
[6]T. Rice, D. Hensel, T. Phillips, and G. Thomas, The Electron-Hole Liquid in a Semiconductor [Russ. transl. Mir, Moscow, 1980].
[7]T. Ando and Y. Murayama, J. Phys. Soc. Jpn. **54**, 1519 (1985).
[8]T. K. Lee, C. S. Ting, and J. J. Quinn, Solid State Commun. **16**, 1309 (1975).
[9]A. A. Abrikosov, Vvedenie v teoriyu normal'nykh metallov (Introduction to the Theory of Normal Metals), Nauka, Moscow, 1972.
[10]N. V. Alkeev, A. S. Kaminskiĭ, and Ya. E. Pokrovskiĭ, Fiz. Tverd. Tela (Leningrad) **18**, 713 (1976) [Sov. Phys. Solid State **18**, 410 (1976)].
[11]A. S. Kaminkskii and Ya. E. Pokrovskiĭ, Zh. Eksp. Teor. Fiz. **76**, 1727 (1979) [Sov. Phys. JETP **49**, 878 (1979)].
[12]C. J. Adkins, S. Pollitt, and M. Pepper, Phys. Rev. Lett. **45**, 494 (1980).
[13]K. von Klitzing, G. Dorda, and M. Pepper, Phys. Rev. Lett. **45**, 494 (1980).
[14]E. I. Rashba and V. B. Timofeev, Fiz. Tekh. Poluprovodn. No. 6 (1986) [Sov. Phys. Semicond. No. 6 (1986)].
[15]I. V. Kukushkin, Zh. Eksp. Teor. Fiz. **84**, 1840 (1983) [Sov. Phys. JETP **57**, 1072 (1983)].
[16]D. C. Tsui, H. L. Stormer, and A. C. Gossard, Phys. Rev. Lett. **50**, 1559 (1982).
[17]R. B. Laughlin, Phys. Rev. Lett. **50**, 1395 (1983).
[18]I. V. Kukushkin and V. B. Timofeev, Zh. Eksp. Teor. Fiz. **89**, 1692 (1985) [Sov. Phys. JETP **62**, 976 (1985)].

Translated by Dave Parsons